Multiple Electrochemical Doping-Induced Insulator-to-Conductor Transitions Observed in the Conjugated Ladder Polymer Polybenzimidazobenzophenanthroline (BBL)[#]

Teketel Yohannes,[†,||] Helmut Neugebauer,[*,†] Silvia Luzzati,[‡] Marinella Catellani,[‡] Samson A. Jenekhe,[§] and N. Serdar Sariciftci[†]

Physical Chemistry, Johannes Kepler University Linz, Altenbergerstrasse 69, A-4040 Linz, Austria, Istituto di Chimica delle Macromolecole, CNR, Via Bassini 15, I-20133 Milano, Italy, and Department of Chemical Engineering, University of Rochester, Rochester, New York 14627-0166

Spectroelectrochemical techniques have been used to study doping-induced reactions in conjugated polymers. Here, we report results on reduction reactions (n-doping) of the conjugated ladder polymer polybenzimidazobenzophenanthroline (BBL). The spectra are recorded in situ during applied potential in a three-electrode spectroelectrochemical cell. The spectral and thus the structural changes during the reduction (n-doping) of the polymer film at different electrode potentials are discussed. In contrast to most of the other conjugated polymers, this polymer shows four reversible redox reactions during n-doping, corresponding to various insulating and conducting forms of BBL.

Introduction

Macromolecular structures with unsaturated (sp[2] hybridized) carbon backbones have attracted much interest in the past decades because of their semiconducting properties as well as the insulator → metal transitions upon oxidation (p-doping) or reduction (p-doping).[1−4] These semiconducting polymers are intrinsically nonconducting materials in their pristine state because of the large band gap (E_g larger than 2 eV). Upon doping, however, mobile quasiparticles such as solitons and polarons are created in the π-electron chain and thus the conductivity jumps orders of magnitude to metallic values.[2,5] The electrical conductivity of conducting polymers can reach 10^4 S/cm, which is nearly temperature independent.[6] This insulator-to-metal transition has been studied in great detail in polyacetylenes and other conjugated, conducting polymers such as polyanilines, polypyrroles, and polythiophenes. In these p-type semiconducting conjugated polymers, the doping-induced insulator-to-metal transition is generally described as a chemical oxidation reaction:

semiconducting polymer (insulator) + oxidant ⇌ conducting polymer[+] (metallic) + oxidant[−]

Polyaniline (PANI) is an exception, and there are two separate consecutive redox reactions observed that are associated with insulator → metal → insulator type tandem reactions.[7] Thus, the fully oxidized (heavily p-doped) state of PANI is an insulator and only the middle oxidized state is a metal.[8]

For applications in optoelectronic devices, like photodetectors, organic solar cells, light-emitting diodes, organic thin-film transistors, or chemical sensors, n-dopable polymers, which show reversible chemical or electrochemical reduction reactions,
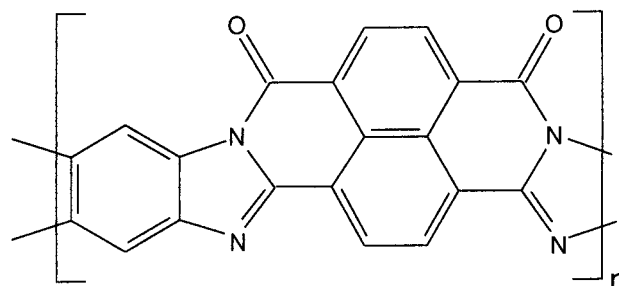
* Corresponding author. FAX +43-732-2468-770; e-mail helmut.neugebauer@jk.uni-linz.ac.at.
† Johannes Kepler University. Linz.
‡ Istituto di Chimica delle Macromole.
§ University of Rochester.
|| Permanent address: Chemistry Department, Bahir Dar Teachers College, Bahir Dar, Ethiopia.
Dedicated to Prof. Fred Wudl on the occasion of his 60th birthday.

Figure 1. Chemical structure of BBL.

are of great importance. The conjugated polymer poly[(7-oxo-7, 10-benz[*de*]-imidazo[4′,5′:5,6] benzimidazo[2,1-*a*] isoquinoline-3, 4:10, 11-tetrayl)-10-carbonyl], abbreviated as BBL (see Figure 1), is a member of a class of materials called ladder polymers, which are double-stranded, highly conjugated macromolecules with rigid chain structure. BBL has high-temperature stability (>500 °C), good mechanical properties (high tensile strength), and exceptional solvent and chemical resistance.[9−11] In addition, BBL has interesting features such as n-type conductivity,[10−14] good photoconductivity,[15] large nonlinear optical properties,[16] and the highest electron affinity value among known n-type semiconducting polymers.[12−14]

BBL in the neutral form is an electrical insulator ($\sigma \approx 10^{-12}$ S/cm).[10,11,17] BBL films can be oxidized or reduced with electron donors or electron acceptors chemically,[10,11] electrochemically,[12,14] or by ion implantation.[18] Kim reported the doping of BBL chemically, with oxidants, reductants, and strong acids, and achieved electrical conductivity as high as 2 S/cm.[10,11] On the other hand, Jenekhe reported the reduction (n-doping) of BBL electrochemically with conductivity as high as 20 S/cm.[14] Thermal annealing of pristine samples was observed to increase the conductivity up to $\sigma \approx 10^{-6}$ S/cm.[10,11] The electronic transport properties of BBL are affected by moisture,[19] thermal treatment,[20,21] and pressure.[22]

BBL is conjugated and can support mobile quasiparticles such as polarons. Experimental and theoretical studies on structural

Electrochemical Doping-Induced Transitions in BBL

J. Phys. Chem. B, Vol. 104, No. 40, 2000 **9431**

changes and redox mechanisms of BBL during reduction have been discussed in the literature.[12,23] Wilbourn and Murray reported that BBL shows two main redox waves during reduction in the cyclic voltammogram using tetrabutylammonium as a cation.[12] However, they mentioned that the cyclic voltammograms are very sensitive to the particular electrolyte cation used, where the two main waves may split into more waves. In another paper, Wilbourn and Murray studied how the conductivity varies with potential during electrochemical reduction of the film. They reported that the BBL conductivity depends on the electrode potential and displays two maxima that differ by about 10 times in conductivity.[13] Unresolved, however, was the issue whether the two maxima observed in the in situ conductivity measurements are associated with distinct redox reactions. Indeed the two consecutive insulator → metal transitions cannot be explained by just two electrochemical processes.

The combination of electrochemical and spectroscopic techniques has been used successfully to study redox reactions in conjugated polymers.[24-30] These techniques are fast and sensitive and are used to probe structural changes and electronic band modifications during the processes. The experiments can be carried out in situ: applying electrode potential and simultaneously monitoring the spectroscopic changes. The vibrational features observed for pristine and doped conjugated polymers are different and are used as signatures for the electronic and the molecular structural changes due to doping. Attenuated total reflection Fourier transform infrared (ATR-FTIR) spectroelectrochemical studies of conjugated polymers have been reported on polypyrrole,[31] PANI,[7,32-35] polythiophene and derivatives,[36-42] and poly-*p*-phenylenevinylene.[43,44]

In this work we present in situ spectroscopic evidence for the existence of four clearly distinct and spectroscopically well-resolved reactions during electrochemical reduction of BBL solid films (n-doping). As such, this is the only conjugated polymer known with four consecutive redox reactions on the main chain.

Experimental Section

Tetrabutylammoniumperchlorate, Bu$_4$NClO$_4$ (Fluka), was dried under vacuum at 130 °C for 2 h before use. Water-free acetonitrile (Merck) was stored over molecular sieve before measurement. Great precaution was taken to protect the electrolyte solution from atmospheric oxygen and water throughout the experiments. The chemical synthesis of BBL was reported elsewhere.[45] Thin films were prepared by spin-coating from a solution of 0.8% BBL in gallium chloride/nitromethane onto glass substrates in laboratory atmosphere. The resulting polymer/Lewis acid complex film was washed with deionized water several times and subsequently placed in fresh deionized water overnight to remove the Lewis acid completely. Using a pair of tweezers the film was peeled off while still wet, yielding a film floating on the water surface. The free-standing film was then transferred onto a germanium reflection element covered with a thin layer of evaporated platinum for FTIR absorption and photoinduced infrared absorption (PIA) measurements, or onto indium-doped tin oxide (ITO), coated glass for UV−vis−near infrared (NIR) and Raman measurements. For electrochemical comparison, films were also transferred onto Pt electrodes. The resulting solid film-covered substrate was dried in a vacuum oven for 6 h at 80 °C.

The ATR-FTIR spectroelectrochemical measurements were carried out in a three-electrode spectroelectrochemical cell with a germanium working electrode, a platinum foil counterelectrode, and a silver wire/silver chloride quasi-reference electrode

in the electrolyte solution. The potential of this reference electrode was determined as −190 mV versus saturated calomel electrode (SCE). All potential values in this paper refer to this reference electrode unless otherwise mentioned. The cell was placed in the FTIR compartment and the instrument was purged with nitrogen continuously throughout the experiment. The electrolyte solution for the in situ spectroelectrochemical experiments was 0.1 M Bu$_4$NClO$_4$ in acetonitrile. A continuous flow system for the electrolyte solution was used where the solution (placed in an external container where it was blanketed with argon after purging for few minutes) flows in and out of the electrochemical cell using Teflon plastic tubes.

To obtain reduction of BBL, a slow potential scan between 0.6 V and −2.0 V with a scan rate of 5 mV/s using a sweep generator Prodis 1/14 I and a potentiostat Jaissle 1002 T-NC was applied to the film. The cyclic voltammogram was recorded on an *x*−*y* recorder. During the scan, in situ FTIR spectra with a resolution of 4 cm^{-1} were measured. To obtain specific spectral changes during individual electrochemical reactions a spectrum just before the considered reaction was chosen as reference. The subsequent spectra were related to this reference spectrum, showing only the spectral differences during the process. The spectra are plotted as $\Delta[-\log(T_{ATR})]$, where T_{ATR} is the transmission in ATR geometry. For each spectrum, 32 interferograms were coadded, covering a range of about 90 mV in the cyclic voltammogram. The potential values given for each reference spectrum in this paper correspond to the mean value of this range. The FTIR and PIA spectra were recorded using a Bruker IFS 66S spectrometer with a mercury−cadmium−telluride detector.

For measuring PIA infrared spectra, the BBL-covered substrate was mounted in a cryostat with ZnSe windows and cooled with liquid nitrogen. The sample was illuminated in 45° geometry through a quartz window of the cryostat by an Ar$^+$ laser (488 nm, 30 mW/cm^2). The PIA infrared spectrum was obtained by measuring 10 single-beam spectra under illumination followed by 10 single-beam spectra taken in the dark. For a better signal-to-noise ratio, 300 repetitions of the measuring sequence were accumulated.

The in situ UV−vis−NIR and Raman spectroelectrochemical measurements were carried out with a modified infrasil cuvette containing an ITO-coated glass working electrode, a platinum wire counterelectrode, and a silver wire reference electrode (−140 mV vs SCE). The measurements have been done using Bu$_4$NClO$_4$ as electrolyte and acetonitrile as a solvent, in dry conditions and under nitrogen atmosphere. The films were reduced potentiostatically, during which the in situ UV−vis−NIR and Raman spectra were recorded at room temperature. The Raman spectra were obtained by exciting with the 514 nm Ar$^+$ laser line, using a Jasco TRS300 triple monochromator with an EG&G intensified diode array. The spectral resolution was 4 cm^{-1}. The in situ UV−vis−NIR absorption spectra were recorded using a Cary 2400 spectrophotometer.

Results and Discussion

Cyclic Voltammetry. The cyclic voltammetric response (CV) for the reduction (n-doping) and reoxidation (undoping) processes of BBL on Ge and, for comparison, on Pt electrodes (in a standard electrochemical cell with SCE reference electrode, separated from the electrolyte solution by a diaphragm to avoid contamination) in Bu$_4$NClO$_4$ containing electrolyte solution are shown in Figure 2. From the CVs four distinct and clearly observable reduction waves were obtained at $E_A \approx -0.6$ V (shoulder), $E_B \approx -0.9$ V (peak), $E_C \approx -1.1$ V (peak), and E_D
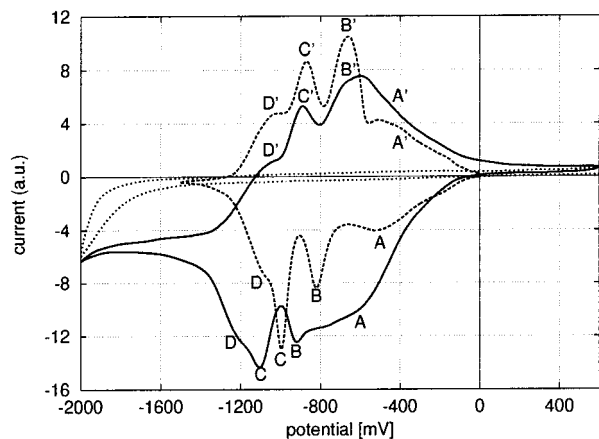
Figure 2. CV for reduction of BBL. Solid line: on a Ge working electrode, Ag/AgCl quasi-reference electrode, scan rate 5 mV/s. Dashed line: on a Pt working electrode, SCE reference electrode, scan rate 2 mV/s. Dotted line: bare Pt electrode, Ag/AgCl quasi-reference electrode, 50 mV/s. The CVs are scaled individually.
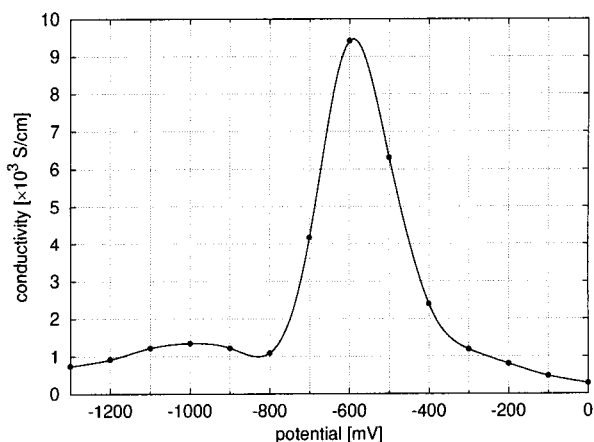

Figure 3. Conductivity measurements of a BBL film in 0.1 M Bu$_4$-NClO$_4$ −acetonitrile electrolyte solution. Data taken from the literature.[13]

≈ -1.2 V (shoulder) using Ge working electrode, and at $E_A \approx -0.52$ V (shoulder), $E_B \approx -0.82$ V (peak), $E_C \approx -1.0$ V (peak), and $E_D \approx -1.1$ V (shoulder) using Pt working electrode. During reoxidation, the corresponding waves were found at $E_{D'} \approx -1.0$ V (shoulder), $E_{C'} \approx -0.89$ V (peak), $E_{B'} \approx -0.61$ V (peak), and $E_{A'} \approx -0.38$ V (shoulder) using Ge working electrode, and at $E_{D'} \approx -1.05$ V (shoulder), $E_{C'} \approx -0.87$ V (peak), $E_{B'} \approx -0.66$ V (peak), and $E_{A'} \approx -0.45$ V (shoulder) using Pt working electrode. The differences in the position of the reduction and reoxidation waves at the two different electrodes is attributed to the differences in electrode material, reference electrode, and scan rate. For comparison, a CV obtained with a bare Pt electrode in the electrolyte solution is also shown in Figure 2. No redox peaks due to the electrolyte solution are found in the range of the BBL redox waves.

Wilbourn and Murray reported that BBL shows only two main redox waves during reduction,[12] in contrast to the four waves obtained in this study. In another paper, Wilbourn and Murray studied how the conductivity varies with potential during electrochemical reduction of BBL.[13] They reported that the conductivity depends on the electrochemical potential and displays two maxima that differ by about 10 times in conductivity (Figure 3). The two consecutive insulator → metal transitions cannot be explained by just two electrochemical reactions. Evidence for the existence of four clearly distinct and spectro-
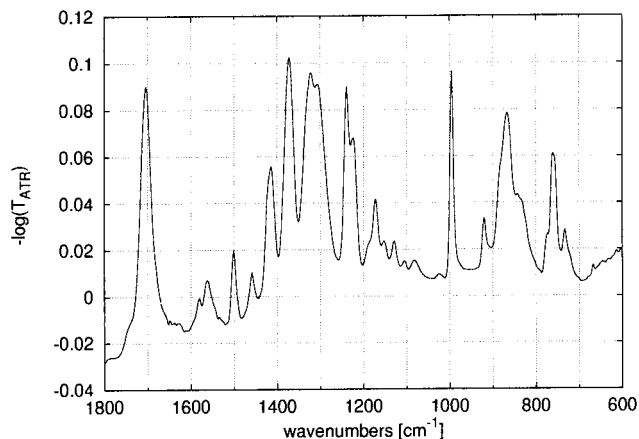

Figure 4. FTIR absorption spectrum of neutral BBL.

TABLE 1: IR Absorption Bands of BBL, Neutral Form (Substance I)

frequency (cm^{-1})	intensity[a]	comment
1745	vw	shoulder
1703	vs	
1647	vw	
1637	vw	
1627	vw	
1609	vw	
1580	w	
1561	m	
1533	vw	
1500	s	
1458	m	
1413	s	
1370	vs	
1320	vs	
1305	vs	shoulder
1237	vs	
1223	s	shoulder
1189	vw	shoulder
1171	s	
1152	w	
1127	m	
1104	w	
1080	m	
1025	w	
995	vs	
919	m	
884	m	shoulder
866	vs	
843	m	shoulder
831	m	shoulder
774	m	shoulder
759	s	
733	m	
719	w	shoulder
668	w	

[a] Intensities: vs, very strong; s, strong; m, medium; w, weak; vw, very weak.

scopically well-resolved reactions during electrochemical reduction of solid BBL films with different reduction states is presented in the next section.

In Situ FTIR Spectroelectrochemistry. Before performing the spectroelectrochemical measurements, the FTIR spectrum of the pristine neutral BBL film (substance I) cast on a germanium reflection element was recorded and is shown in Figure 4 for the frequency region 1800−600 cm^{-1}. In Table 1, frequencies and intensities of the infrared absorption bands of neutral BBL are listed, which are in agreement with previously reported spectra.[11,45,46]
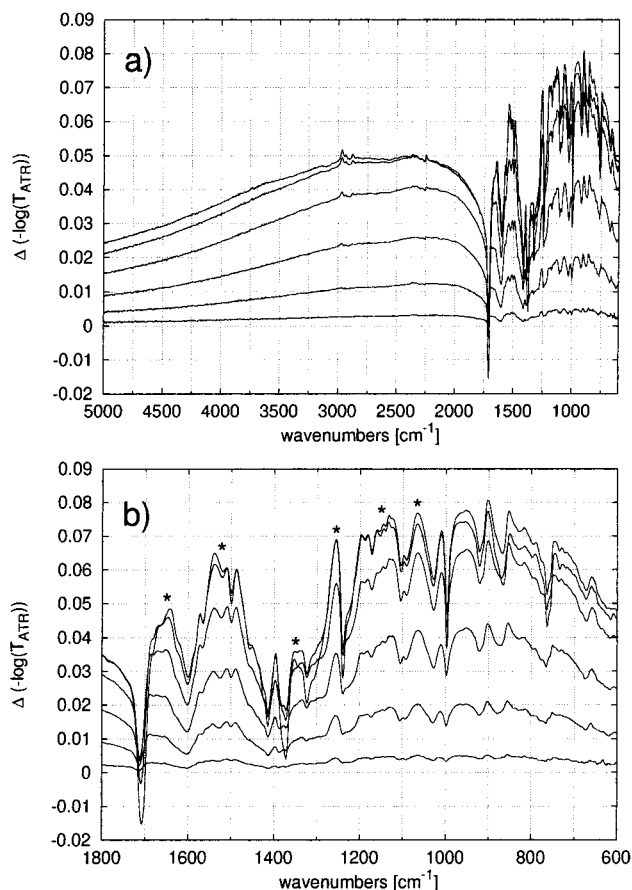
Electrochemical Doping-Induced Transitions in BBL

J. Phys. Chem. B, Vol. 104, No. 40, 2000 **9433**

Figure 5. (a) Difference in situ ATR-FTIR absorption spectra during reduction process A for potentials from −95 mV to −618 mV. Reference spectrum taken around −48 mV. (b) Spectra of (a) in an extended scale.

TABLE 2: IR Bands of Substance II Appearing during First Reduction Process A

frequency (cm^{-1})	intensity[a]	comment
1649	s	sharp
1522	s	broad
1349	m	sharp
1255	s	sharp
1150	s	broad
1066	s	sharp

[a] Intensities: s, strong; m, medium.

The spectral changes during the electrochemical redox reactions were studied using in situ FTIR spectroscopy. Figure 5 shows the difference spectra of BBL during the first reduction process (wave A). As can be seen from Figure 5a, a broad absorption band with absorption maximum above 2000 cm^{-1} appears. This broad absorption comes from an electronic transition involving polaronic states[47−49] and is correlated with an increase in conductivity, where the neutral insulating polymer (substance I) is transformed into an electrically conducting polymer (substance II). The vibrational part of the spectra is depicted in Figure 5b in an extended scale. Usually, vibrational spectra of conjugated polymers are strongly affected by the doping (redox) processes because of strong electron−phonon coupling,[47−49] and the infrared spectra are dominated by new intense bands called infrared active vibration (IRAV) bands. IRAV bands of BBL, appearing during wave A, are marked by asterisks in Figure 5b and are listed in Table 2 with their relative intensities. These growing IRAV bands indicate the formation of substance II. On the other hand, the intensity of the bands at
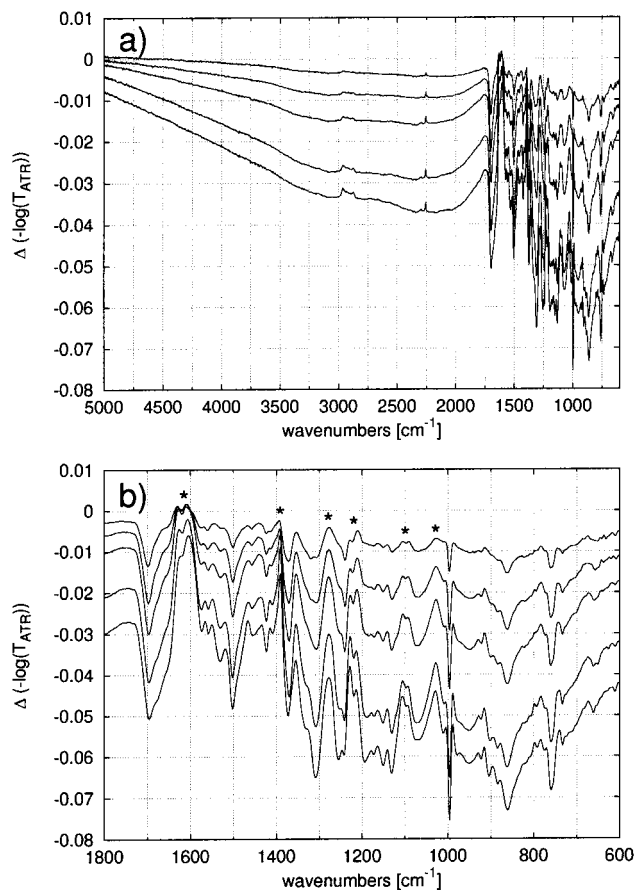

Figure 6. (a) Difference in situ ATR-FTIR absorption spectra during reduction process B for potentials from −618 mV to −1039 mV. Reference spectrum taken around −572 mV. (b) Spectra of (a) in an extended scale.

TABLE 3: IR Bands of Substance III Appearing during Second Reduction Process B

frequency (cm^{-1})	intensity[a]	comment
1614	m	broad
1390	m	sharp
1278	s	
1219	s	doublet
1099	s	doublet
1028	s	sharp

[a] Intensities: s, strong; m, medium.

1703, 1561, 1500, 1458, 1413, 1370, 1320, 1305, 1237, 1171, 995, 866, and 759 cm^{-1} of the neutral substance I decreases because of the conversion into substance II.

Figure 6 shows the difference in situ spectra during the second reduction process (wave B). The broad negative band at high energy (Figure 6a) indicates the formation of a new substance III with low conductivity. In Figure 6b the spectra in an extended scale are depicted. Further decrease in the intensities of substance I and decrease in intensities of substance II together with an increase of sharper bands indicated by asterisks in Figure 6b are observed (formation of substance III). In Table 3 the frequencies and intensities of these increasing bands of substance III are listed. The sharpness of the bands is further suggesting a decrease of conductivity.

Figure 7 depicts the difference in situ FTIR spectra during the third reduction process (wave C). The increase of the broad absorption band above 2000 cm^{-1} (but smaller than in the first reduction process A) with a decrease in applied potential indicates again the increase in conductivity of the film. This
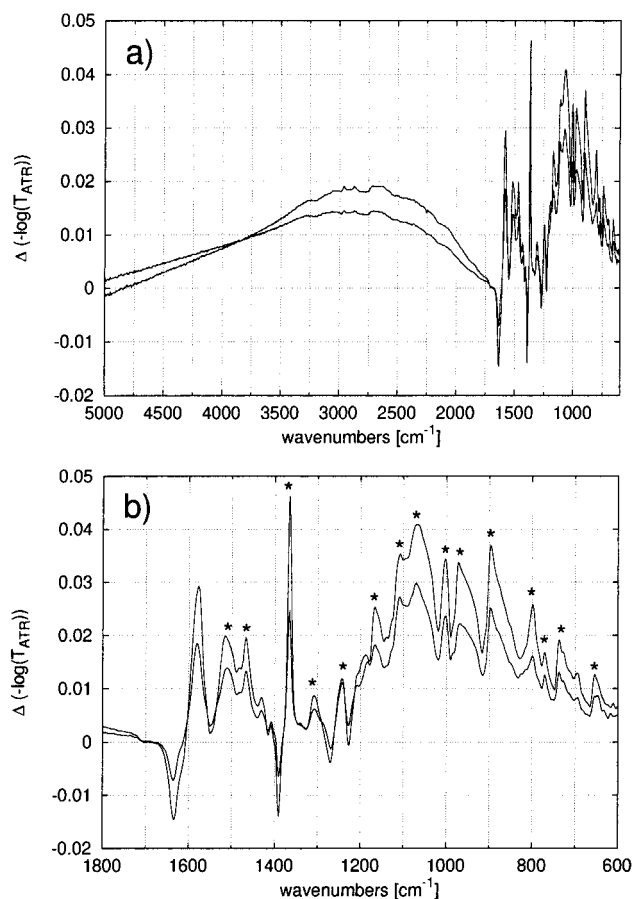
Figure 7. (a) Difference in situ ATR-FTIR absorption spectra during reduction process C for potentials from −1039 mV to −1206 mV. Reference spectrum taken around −996 mV. (b) Spectra of (a) in an extended scale.

TABLE 4: IR Bands of Substance IV Appearing during Third Reduction Process C

frequency (cm^{-1})	intensity[a]	comment
1509	m	sharp
1466	m	sharp
1369	vs	sharp
1312	w	
1240	m	sharp
1168	m	sharp
1109	s	shoulder
1070	s	
1002	s	sharp
968	s	sharp
896	s	sharp
801	m	sharp
771	w	sharp
732	m	sharp
654	m	sharp

[a] Intensities: vs, very strong; s, strong; m, medium; w, weak.

smaller electronic band increase observed in this step (compared with wave A) is in agreement with the small increase in conductivity (Figure 3). The vibrational part of the spectra in an extended frequency scale is shown in Figure 7b. Decrease of bands of substance III and increase of IRAV bands are observed (indicated by asterisks in Figure 7b). In Table 4 the frequencies and intensities of the bands of substance IV are listed. The IRAV bands in the third reduction process C show lower intensities compared with IRAV bands in the first reduction process A. In addition, the bands are sharper than in process A. The lower intensities and the sharper IRAV bands indicate
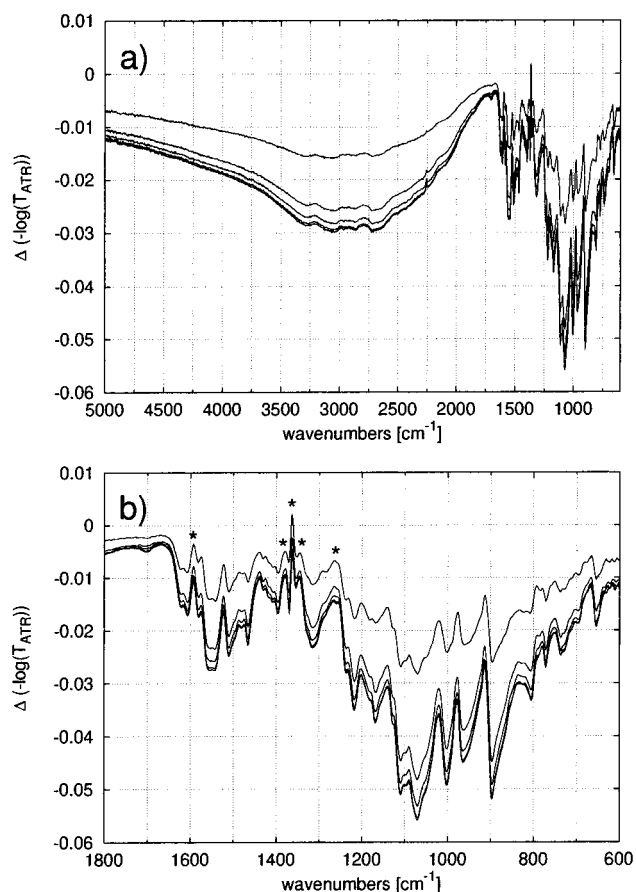

Figure 8. (a) Difference in situ ATR-FTIR absorption spectra during reduction process D for potentials from −1206 mV to −1634 mV. Reference spectrum taken around −1164 mV. (b) Spectra of (a) in an extended scale.

TABLE 5: IR Bands of Substance V Appearing during Fourth Reduction Process D

frequency (cm^{-1})	intensity[a]	comment
1593	m	sharp
1379	m	shoulder
1363	s	sharp
1345	m	shoulder
1261	w	broad

[a] Intensities: s, strong; m, medium; w, weak.

that the delocalization of the negative charges on the chain is rather low in substance IV as compared with substance II.

In Figure 8 the spectra for the fourth reduction process (wave D) are shown. A decrease in the electronic band at high energy is observed with increasing doping level. This decrease is again an indication of the decrease in the conductivity of the film. The spectra in an extended scale are shown in Figure 8b. Decrease in the vibrational bands of substance IV and increase in few new sharp bands (indicated by asterisks in Figure 8b) are observed, which are assigned to substance V (listed in Table 5).

From the in situ FTIR measurements one can clearly see the transition to different states when going in the direction from positive to negative potentials: insulator → conductor → insulator → conductor → insulator, in agreement with the conductivity measurements.[13] Exact reverse processes are found when going back from negative to positive potentials where the difference spectra obtained during the reoxidation processes (waves D′−A′) reverse the spectra of the corresponding reduction processes (waves A−D).
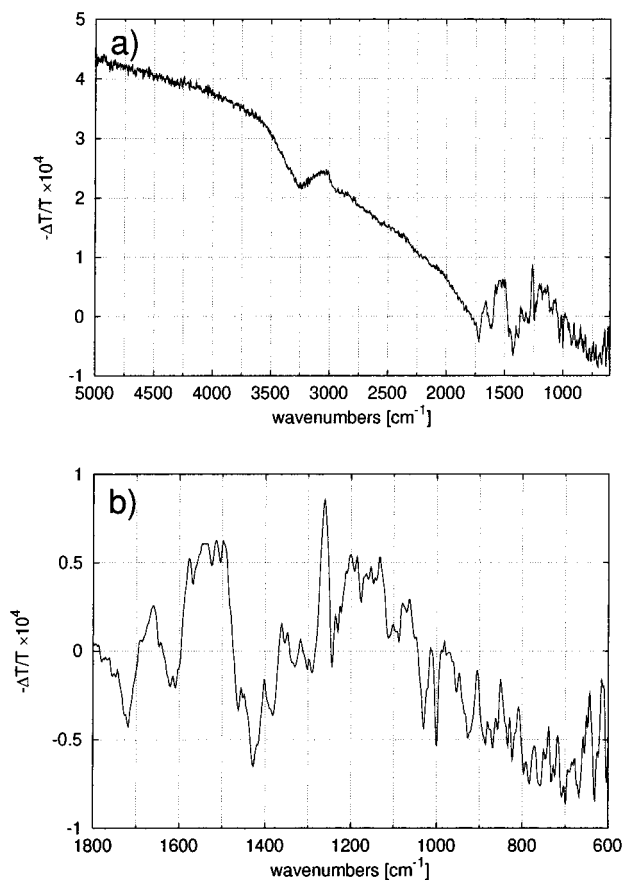
Electrochemical Doping-Induced Transitions in BBL

J. Phys. Chem. B, Vol. 104, No. 40, 2000 **9435**

Figure 9. (a) PIA infrared absorption spectrum of neutral BBL. (b) Spectrum of (a) in an extended scale.

Figure 10. In situ Raman spectra of BBL during reduction at various electrode potentials. 1, 0 mV; 2, -300 mV; 3, -430 mV; 4, -560 mV; 5, -690 mV; 6, -820 mV; 7, -950 mV; 8, -1080 mV; 9, -1210 mV. Excitation wavelength at 514 nm.

Figure 11. In situ optical absorption spectra of BBL during reduction at various electrode potentials. Isosbestic points are marked A, B, and C.

Wilbourn and Murray proposed a reaction scheme for the reduction processes of BBL in acetonitrile leading to quino-dimethanelike structures that are strongly resonance-stabilized with decreasing C=O oscillator strength.[12] From the in situ FTIR spectral measurements we observe a decrease of the band at 1703 cm^{-1} (C=O) of the neutral BBL film even at the first reduction process A suggesting the formation of a similar resonance structure even at a low doping level. To clarify the change in the chemical structures during the reduction processes more structural studies are needed because of the complex nature of the molecule.

Photoinduced FTIR Spectroscopy. When a conjugated polymer film is excited by illumination with light of photon energy higher than the value of the electronic band gap, mobile quasiparticles are produced that give rise to new states in the gap.[2,3,47,48] This method of photodoping is a clean way (compared with chemical and electrochemical doping) of injecting charges onto the polymer chain. The PIA spectrum of a BBL film is shown in Figure 9a for the frequency region 5000−600 cm^{-1}. A broad electronic band in the higher energy region occurs (the spectral feature around 3500−3000 cm^{-1} is due to spectral incompensation during the measurement procedure). Figure 9b shows the spectrum in the extended frequency region between 1800 and 600 cm^{-1}. The appearance of vibrational IRAV bands is observed. The photoinduced IRAV band positions are almost the same as the IRAV bands obtained at low electrochemical n-doping (process A, Figure 4b).

In Situ Raman Spectroelectrochemistry. In addition to infrared spectroscopy, Raman spectroscopy is a useful tool to probe the structural and electronic properties of conjugated polymers. In situ Raman spectra of BBL were measured during
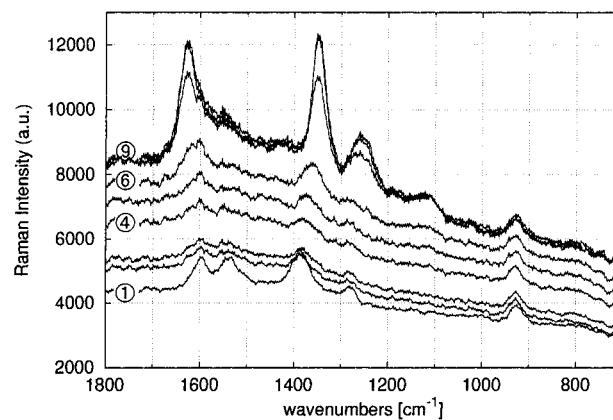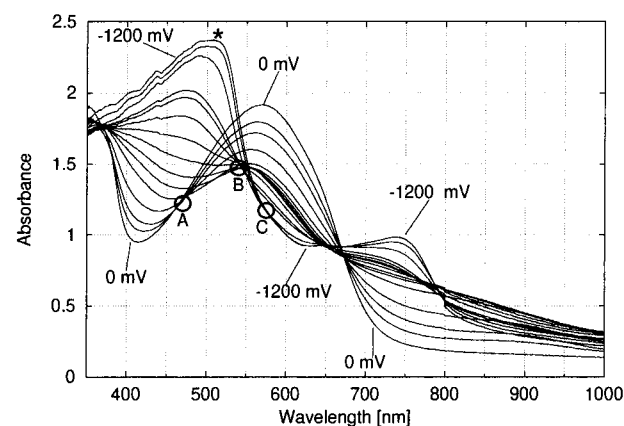
the reduction reactions with excitation at 514 nm. The spectra of the various reduction states are shown in Figure 10. The Raman spectrum of the neutral BBL film (spectrum 1) in contact with the electrolyte solution consists of five main bands at 1597, 1539, 1389, 1282, and 926 cm^{-1} (the band at 926 cm^{-1} comes from the electrolyte). Also from the in situ Raman spectra of BBL the four processes, observed in the in situ FTIR spectro-electrochemical studies, can be distinguished. A decrease of the Raman bands (spectra 2 and 3) corresponds with the first process A. As the applied potential decreases, additional bands at 1627 cm^{-1} (as a shoulder) and at 1125 cm^{-1} start to appear and the band at 1389 cm^{-1} shifts to 1360 cm^{-1} (spectrum 6, process B). By further decrease of the potential, sharp bands at 1627, 1346, and 1258 cm^{-1} appear (spectra 7−9, process C). These main features start decreasing at an applied potential more negative than -1340 mV (not shown in Figure 10, process D).
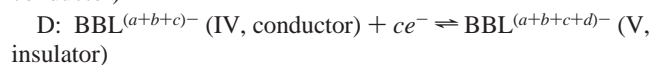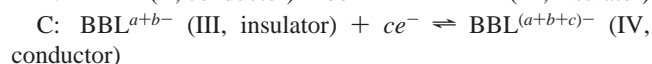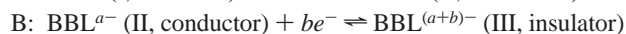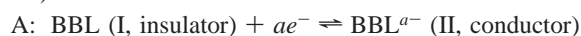
The in situ Raman spectroelectrochemical results can be correlated with UV−vis−NIR optical absorption measurements. Figure 11 shows in situ UV−vis−NIR absorption spectra at different electrode potentials. The wavelength used for the Raman excitation (514 nm) is indicated with an asterisk in the figure. The optical absorption band at 571 nm, assigned to the $\pi-\pi$ transition, starts decreasing continuously as the reduction proceeds while new bands appear. The decrease in the Raman bands of the neutral BBL film in process A corresponds to a decrease in the optical absorption band at 571 nm because the Raman excitation energy is partly in resonance with this

absorption. Because of resonance, the strong Raman band increase in process C can be correlated with an increase in the optical absorption at 510 nm (shoulder on the band at 480 nm). The three processes A, B, and C can also be seen by isosbestic points in the spectra. No isosbestic point for process D was found, probably because of very small spectral changes in the potential range studied.

Conclusion

We proved and found four distinct and spectroscopically well-resolved redox processes during electrochemical reduction (n-doping) of BBL involving five redox states with different conductivities. Because of the complex nature of the polymer, the changes of the chemical structure during the reduction processes have not been precisely determined by this study. However, it is possible to compare our data with the reaction scheme previously proposed for BBL in acetonitrile.[12] This scheme suggests the formation of quinodimethane resonance structures at a very high doping level. Our data indicate the presence of this type of resonance structure even at low doping levels.

In correlation with the in situ electrical conductivity data[13] the four reactions are given in the following reaction scheme (in that scheme BBL refers to one repetitive unit in the polymer chain).

A: BBL (I, insulator) $+ ae^- \rightleftharpoons BBL^{a-}$ (II, conductor)

B: BBL^{a-} (II, conductor) $+ be^- \rightleftharpoons BBL^{(a+b)-}$ (III, insulator)

C: BBL^{a+b-} (III, insulator) $+ ce^- \rightleftharpoons BBL^{(a+b+c)-}$ (IV, conductor)

D: $BBL^{(a+b+c)-}$ (IV, conductor) $+ ce^- \rightleftharpoons BBL^{(a+b+c+d)-}$ (V, insulator)

The overall absolute charge during the reduction process was determined with coulometric assay to be equivalent to a consumption of one electron per BBL monomer unit[12] ($a + b + c + d = 1$ in the reaction scheme above). Although the exact determination of the charges involved in the individual reduction steps is hindered by the overlapping peaks in the CV, the corresponding charges Q in steps A–D can be estimated as $Q_a \approx 0.25e^-$, $Q_b \approx 0.25e^-$, $Q_c \approx 0.35e^-$, and $Q_d \approx 0.15e^-$, respectively. As such, BBL with these unusual n-doping properties is an interesting candidate for applications in opto-electronic devices.[50-52]

References and Notes

(1) Heeger, A. J.; Kivelson, S.; Schrieffer, J. R.; Su, W. P. *Rev. Mod. Phys.* **1988**, *60*, 781.

(2) See for example *Handbook of Conducting Polymers*; 2nd ed.; Skotheim, T. A., Elsenbaumer, R. L., Reynolds J. R., Eds.; Marcel Dekker: New York, 1998.

(3) See for example *Handbook of Organic Conductive Molecules and Polymers*; Nalwa, H. S., Ed.; Wiley: Chichester, 1997; Vol. 1–4.

(4) See for example *Synth. Met. 84–86* (Proceedings ICSM '96) and *Synth. Met. 101–103* (Proceedings ICSM '98).

(5) Su, W. P.; Schrieffer, J. R.; Heeger, A. J. *Phys. Rev. Lett.* **1979**, *42*, 1698.

(6) Menon, R. In *Handbook of Organic Conductive Molecules and Polymers*; Nalwa, H. S., Ed.; Wiley: Chichester, 1997; Vol. 4, p 47.

(7) Kuzmany, H.; Sariciftci, N. S.; Neugebauer, H.; Neckel, A. *Phys. Rev. Lett.* **1988**, *60*, 212.

(8) MacDiarmid, A. G.; Chiang, J. C.; Richter, A. F.; Epstein, A. J. *Synth. Met.* **1987**, *18*, 285.

(9) Arnold, F. E.; Van Deusen, R. L. *J. Appl. Polym. Sci.* **1971**, *15*, 2035.

(10) Kim, O.-K. *J. Polym. Sci., Polym. Lett. Ed.* **1982**, *20*, 663.

(11) Kim, O.-K. *Mol. Cryst. Liq. Cryst.* **1984**, *105*, 161.

(12) Wilbourn, K.; Murray, R. W. *Macromolecules* **1988**, *21*, 89.

(13) Wilbourn, K.; Murray, R. W. *J. Phys. Chem.* **1988**, *92*, 3642.

(14) Jenekhe, S. A. *Polym. Mater. Sci. Eng.* **1989**, *60*, 419.

(15) Antoniadis, H.; Abkowitz, M. A.; Osaheni, J. A.; Jenekhe, S. A.; Stolka, M. *Synth. Met.* **1993**, *60*, 149.

(16) Jenekhe, S. A.; Roberts, M. F.; Agrawal, A. K.; Meth, J. S.; Vanherzeele, H. *Mater. Res. Soc. Proc.* **1991**, *214*, 55.

(17) Coter, F.; Belaish, Y.; Davidov, D.; Dalton, L. R.; Ehrenfreund, E.; Mclean, M. R.; Nalwa, H. S. *Synth. Met.* **1989**, *29*, E471.

(18) Jenekhe, S. A.; Tibbetts, S. A. *J. Polym. Sci. Part B Polym. Phys.* **1988**, *26*, 201.

(19) Antoniadis, H.; Abkowitz, M. A.; Osaheni, J. A.; Jenekhe, S. A.; Stolka, M. *Chem. Mater.* **1994**, *6*, 63.

(20) Wang, C. S.; Lee, C. Y. C.; Arnold, F. E. *Mater. Res. Soc. Proc.* **1992**, *247*, 747.

(21) Narayan, K. S.; Long, S. M.; Epstein, A. J.; Taylor, B. E.; Spry, R. J.; Bai, S. J.; Wang, C. S. *Bull. Am. Phys. Soc.* **1993**, *38*, 110.

(22) Narayan, K. S.; Singh, A. K.; Ramasesha, S. K. *J. Phys. D: Appl. Phys.* **1997**, *30*, L16.

(23) Hong, S. Y.; Kertesz, M.; Lee, Y. S.; Kim, O.-K. *Macromolecules* **1992**, *25*, 5424.

(24) Orata, D.; Buttry, D. A. *J. Am. Chem. Soc.* **1987**, *109*, 3574.

(25) Geniès, E. M.; Lapkowski, M. *J. Electroanal. Chem.* **1987**, *236*, 199.

(26) Kessel, R.; Hansen, G.; Schultze, J. W. *Ber. Bunsen-Ges. Phys. Chem.* **1988**, *92*, 710.

(27) Barbero, C.; Miras, M. C.; Haas, O.; Kötz, R. *J. Electrochem. Soc.* **1991**, *138*, 669.

(28) Neugebauer, H.; Ping, Z. *Mikrochim. Acta (Suppl.)* **1997**, *14*, 125.

(29) Neugebauer, H. *Macromol. Symp.* **1995**, *94*, 61.

(30) Zagorska, M.; Pron, A.; Lefrant, S. In *Handbook of Organic Conductive Molecules and Polymers*; Nalwa, H. S., Ed.; Wiley: Chichester, 1997; Vol. 3, p 183.

(31) Neugebauer, H.; Sariciftci, N. S. In *Lower Dimensional Systems and Molecular Electronics*; Nato ASI series, Series B: Physics; Metzger, R. M., Day, P., Papavassiliou, G. C., Eds.; Plenum Press: New York, 1991; Vol. 248, p 401.

(32) Moser, A.; Neugebauer, H.; Maurer, K.; Theiner, J.; Neckel, A. In *Electronic Properties of Conjugated Polymers*; Springer Series in Solid-State Sciences; Kuzmany, H., Mehring, M., Roth, S., Eds.; Springer: Berlin, 1992; Vol. 107, p 276.

(33) Neugebauer, H.; Sariciftci, N. S.; Kuzmany, H.; Neckel, A. In *Electronic Properties of Conjugated Polymers III*; Springer Series in Solid-State Sciences; Kuzmany, H., Mehring, M., Roth, S., Eds.; Springer: Berlin, 1989; Vol. 91, p 315.

(34) Sariciftci, N. S.; Kuzmany, H.; Neugebauer, H.; Neckel, A. *J. Chem. Phys.* **1990**, *92*, 4530.

(35) Ping, Z.; Neugebauer, H.; Neckel, A. *Electrochim. Acta* **1996**, *41*, 767.

(36) Neugebauer, H.; Nauer, G.; Neckel, A.; Tourillon, G.; Garnier, F.; Lang, P. *J. Phys. Chem.* **1984**, *88*, 652.

(37) Neugebauer, H.; Neckel, A.; Brinda-Konopik, N. In *Electronic Properties of Conjugated Polymers and Related Compounds*; Springer Series in Solid-State Sciences; Kuzmany, H., Mehring, M., Roth, S., Eds.; Springer: Berlin, 1985; Vol. 63, p 227.

(38) Sariciftci, N. S.; Kolbert, A. C.; Mehring, M.; Gaudl, K. U.; Bäuerle, P.; Neugebauer, H.; Neckel, A. *Chem. Phys. Lett.* **1991**, *182*, 326.

(39) Sariciftci, N. S.; Mehring, M.; Gaudl, K. U.; Bäuerle, P.; Neugebauer, H.; Neckel, A. *J. Chem. Phys.* **1992**, *96*, 7164.

(40) Neugebauer, H.; Kvarnström, C.; Brabec, C.; Sariciftci, N. S.; Kiebooms, R.; Wudl, F.; Luzzati, S. *J. Chem. Phys.* **1999**, *110*, 12108.

(41) Kvarnström, C.; Neugebauer, H.; Blomquist, S.; Ahonen, H. J.; Kankare, J.; Ivaska, A. *Electrochim. Acta* **1999**, *44*, 2739.

(42) Kvarnström, C.; Neugebauer, H.; Ivaska, A.; Sariciftci, N. S. *J. Mol. Struct.*, (in press).

(43) Neugebauer, H.; Sariciftci, N. S.; Srinivasan, S. *Synth. Met.* **1997**, *84*, 635.

Electrochemical Doping-Induced Transitions in BBL

J. Phys. Chem. B, Vol. 104, No. 40, 2000 **9437**

(44) Neugebauer, H.; Srinivasan, S.; Tasch, S.; Leising, G.; Sariciftci, N. S. *Proc. SPIE-Int. Soc. Opt. Eng.* **1997**, *3145*, 507.

(45) Jenekhe, S. A.; Johnson, P. O. *Macromolecules* **1990**, *23*, 4419.

(46) Arnold, F. E.; Van Deusen, R. L. *Macromolecules* **1969**, *2*, 497.

(47) Gussoni, M.; Castiglioni, C.; Zerbi, G. In *Spectroscopy of Advanced Materials*; Clark, R. J. H., Hester, R. E., Eds.; Wiley: New York, 1991; p 251.

(48) Zerbi, G.; Gussoni, M.; Castiglioni, C. In *Conjugated Polymers*; Brédas, J. L., Silbey, R., Eds.; Kluwer: Dordrecht, 1991; p 435.

(49) Del Zoppo, M.; Castiglioni, C.; Zuliani, P.; Zerbi, G. In *Handbook of Conducting Polymers*, 2nd ed.; Skotheim, T. A., Elsenbaumer, R. L., Reynolds J. R., Eds.; Marcel Dekker: New York, 1998; p 765.

(50) Chen, X. L.; Jenekhe, S. A. *Macromolecules* **1997**, *30*, 1728.

(51) Jenekhe, S. A.; de Paor, L. R.; Chen, X. L.; Tarkka, R. M. *Chem. Mater.* **1996**, *8*, 2401.

(52) Osaheni, J. A.; Jenekhe, S. A.; Perlstein, J. *J. Phys. Chem.* **1994**, *98*, 12727.